Journal of Engineering Research and Reports

Volume 27, Issue 8, Page 14-32, 2025; Article no.JERR.140958
ISSN: 2582-2926

Mathematical Modeling of Mass and Heat Transfer in a Dehumidifying Plastic Dryer

Anthony A. Adeyanju [a*]

[a] *Department of Mechanical and Manufacturing Engineering, The University of the West Indies, St. Augustine Campus, Trinidad.*

Author's contribution

The sole author designed, analyzed, interpreted and prepared the manuscript.

Article Information

DOI: https://doi.org/10.9734/jerr/2025/v27i81592

Open Peer Review History:
This journal follows the Advanced Open Peer Review policy. Identity of the Reviewers, Editor(s) and additional Reviewers, peer review comments, different versions of the manuscript, comments of the editors, etc are available here: https://pr.sdiarticle5.com/review-history/140958

Original Research Article

Received: 26/05/2025
Published: 02/08/2025

ABSTRACT

The dehumidification of plastic resins is an essential process aimed at mitigating the adverse effects of excessive or insufficient moisture content during thermal processing operations such as molding and extrusion. The extent to which moisture compromises the structural integrity and performance of the final product is contingent upon the specific characteristics of the polymer and its end-use application. Nevertheless, inadequate or incomplete drying of the raw material invariably introduces defects either during fabrication or in subsequent service conditions. In this study, a theoretical framework is developed to analyze the coupled heat and mass transfer phenomena occurring within a dehumidifying dryer operating under steady-state conditions. The model considers a drying bed partially occupied by a porous desiccant medium, with a closed-form analytical solution derived based on the interplay between the geometric configuration of the flow channel, the physicochemical properties of the desiccant, and the interphase mass transfer dynamics within the porous matrix. Additionally, the investigation encompasses the evaluation of moisture-loss behavior and the influence of airflow characteristics within the drying hopper—

**Corresponding author: Email: Anthony.adeyanju@sta.uwi.edu, anthony.adeyanju@uwi.edu;*

Cite as: *Adeyanju, Anthony A. 2025. "Mathematical Modeling of Mass and Heat Transfer in a Dehumidifying Plastic Dryer". Journal of Engineering Research and Reports 27 (8):14-32. https://doi.org/10.9734/jerr/2025/v27i81592.*

parameters deemed critical to the drying kinetics. The analysis underscores the necessity of maintaining a sufficiently high and uniform airflow to ensure that plastic pellets attain and sustain the target drying temperature for the requisite residence time, thereby facilitating effective moisture extraction and enhancing overall process reliability.

Keywords: Heat and Mass Transfer; dehumidifying dryer; porous desiccant medium; steady-state analysis; closed-form modeling.

NOMENCLATURE

where,

t_c = Thickness of the Dehumidify Bed channel

t_{po} = Thickness of porous medium

C_P = Specific heat at constant pressure

D_{v-a} = Water vapour-air mass diffusivity

$D_{po(v-a)}$ = Porous media water vapour-air mass diffusivity i

Δp = pressure gradient (-ve)

Q_{ad} = Heat of adsorption

K = Thermal conductivity

T = Temperature

t = Time

C_1, C_2 = Equillibrium conditions

x, y = coordinates

m_d = desiccant moisture content

q = Internal heat rate

q_L " = bed lower surface heat flux

q_U " = bed upper surface heat flux

$\dot{m}_{wv}$ = Rate of production of water vapour

$\dot{M}_{wv}$ = Rate of production of water vapour(dimensionless)

Sh = Sherwood number (dimensionless)

St_m = mass transfer - Stanton number (dimensionless)

m = water vapour mass fraction

$\dot{q}$ = Internal heat rate (dimensionless)

u = velocity

u_b = bulk velocity

1. INTRODUCTION

The continuous growth of the global population, along with rising standards of living, has significantly increased the demand for advanced, energy-efficient, and environmentally sustainable drying technologies. Predicting the future trajectory of drying technology remains complex, primarily due to the dynamic interplay between technological innovation and environmental

regulations. Historically, the most significant breakthroughs occurred between 1978 and 1988; however, recent developments have been propelled by stricter energy efficiency mandates, growing environmental awareness, the integration of renewable energy sources, and consumer demand for high-quality products with minimized life-cycle costs (Mujumdar, 2007). Drying operations are inherently energy-intensive and are critical across multiple industrial sectors such as plastics, food processing, textiles, paper production, and chemical manufacturing. In many of these industries, drying accounts for the highest operational energy costs, often exceeding the initial capital costs of the equipment. For instance, the papermaking industry dedicates up to 35% of its energy consumption to drying processes, while the chemical sector may require less than 5% (Keey, 1992). Furthermore, the energy efficiency of conventional drying systems typically ranges from 20% to 60%, largely dependent on dryer configuration and material properties (Strumillo & Kudra, 1986). Recent studies have emphasized the urgency of improving drying efficiency through technological integration and sustainability metrics. Martynenko and Vieira (2023) introduced a 4E-based framework—evaluating energy, exergy, environmental, and economic performance—to quantify the sustainability of food drying technologies. Similarly, Ying and Spang (2024) reviewed drying techniques for grains, fruits, and vegetables, concluding that hybrid systems combining solar, microwave, and infrared sources offer the lowest payback periods and highest energy efficiencies. Moreover, Santos et al. (2025) conducted a bibliometric analysis highlighting the shift toward drying systems that preserve bioactive compounds, use sustainable materials, and incorporate intelligent control systems. Desiccant-assisted drying and dehumidification systems have emerged as viable alternatives, particularly when integrated into hybrid configurations. De Antonellis et al. (2012) developed a simulation model to evaluate the energy performance of hybrid drying systems that incorporate desiccant wheels, analyzing various configurations to optimize control strategies and reduce energy consumption. Loemba (2022) further demonstrated that heat pump dryers can reduce energy consumption by up to 80%, achieving specific moisture extraction rates of 9.25 kg/kWh and coefficients of performance ranging from 1.94 to 5.34. Parallel to system-level improvements, significant research has focused on modeling mass transfer within desiccant materials. Internal resistance to mass diffusion is a major limiting factor in desiccant performance, necessitating accurate modeling approaches. Notable theoretical models include the Pseudo-Gas-Side Controlled Model (Ruivo et al., 2009), Surface Diffusion Resistance Model (Rigby, 2025), Solid-Side Resistance Model (Wong and Park, 2016), and the Parabolic Concentration Profile Model (Cuče, et al, 2025). While each model offers valuable insights, their predictive accuracy varies significantly under transient or cyclic drying conditions. Longo and Gasparella, 2005 analyzed a dual-column silica gel dehumidification system, applying the Solid-Side Resistance model to simulate cyclic adsorption-desorption behavior and identifying fluid friction as a critical factor affecting heat and mass transfer. Likewise, Ge et al., (2008) employed finite difference methods to simulate rotary desiccant wheels, focusing on desiccant characteristics such as isotherm shape, sorption hysteresis, and thermal capacity. More recently, a comprehensive review by the *Journal of Thermal Analysis and Calorimetry* (2025) examined rotary desiccant wheels for smart building HVAC systems, reporting regeneration COP values of 0.3–0.4 at 50 °C and moisture removal rates up to 4.55 kg/kg of dry air at flow rates of 2 m/s. In the field of plastic manufacturing, precise control of drying parameters—including drying temperature, duration, air velocity, and vapor content—is essential to ensure product integrity and reduce energy waste. This study presents a mathematical model that simulates the dehumidification behaviour of plastic pellets, taking into account the coupled heat and mass transfer processes, desiccant medium dynamics, and airflow characteristics. Such modeling is critical for optimizing drying performance and maintaining consistent moisture levels during extrusion and moulding operations.

2. CREATION OF PLASTIC PELLETS

Plastic pellets—commonly derived from petroleum-based feedstocks—are fundamental raw materials extensively utilized in the fabrication of plastic containers, bottles, and molded components. These pellets typically exist in either an amorphous transparent state or a semi-crystalline form, which often presents as a milky-white opaque material (Longo and Gasparella, 2005). A key property governing the utility of plastic pellets is **intrinsic viscosity (IV)**, which serves as a proxy for the average

molecular weight and chain length of the polymer. The performance characteristics of the final product—such as mechanical strength, thermal resistance, and processability—are directly correlated with IV. Higher intrinsic viscosity reflects longer polymer chains, leading to superior end-use properties. Consequently, the preservation of intrinsic viscosity during thermal and mechanical processing is essential. The most frequent cause of IV degradation is the presence of moisture within the pellet matrix, which facilitates **hydrolytic degradation** during melt processing (Jurinak, 1984). Due to their **lipophilic** nature, plastic pellets exhibit a strong affinity for organic compounds present in aquatic environments, readily adsorbing toxicants from seawater onto their surfaces. This phenomenon renders them vulnerable to contamination by **persistent organic pollutants (POPs)—** including polychlorinated biphenyls (PCBs), dichlorodiphenyltrichloroethane (DDT), and polycyclic aromatic hydrocarbons (PAHs)—which can accumulate in concentrations up to one million times higher than that of the surrounding water (Rios et al., 2007). These pollutants, many of which are bioaccumulative and carcinogenic, pose severe ecological and public health risks (Mato et al., 2001). In addition to environmental adsorption, various **additives** are incorporated during manufacturing to modify the pellet's properties. For instance, **Nonylphenol (NP)** is frequently used as a plasticizer and antioxidant but is now recognized for its endocrine-disrupting potential (Talsness et al., 2009). The production of plastic pellets is conducted exclusively at industrial scale, employing precise thermal conditioning protocols. Typically, the polymer resin is **dehumidified at 120 °C for approximately 5 hours** to ensure sufficient moisture removal without inducing polymer chain scission. Thereafter, the dried material is introduced into an **extrusion barrel operating at approximately 260 °C**, which facilitates melt processing and formation of uniform pellets with diameters ranging from 2 mm to 3 mm (Longo and Gasparella, 2005). The choice of dehumidification temperature is critical: while higher temperatures would accelerate drying, they risk degrading molecular integrity. Similarly, the extrusion temperature must closely align with the polymer's melting point to enhance processability while mitigating thermal degradation. Conventional recycling methods—such as injection moulding or mechanical pelletizing—often suffer from **progressive deterioration of material properties**, particularly when polymers are repeatedly subjected to thermal cycling. Each remelting event contributes to the breakdown of polymer chains, and if conducted at excessively high temperatures or repeated too frequently, the resultant material may lose structural viability (Jurinak, 1984). To minimize this, the **Poly Pelletizer** was designed to operate near the polymer's melting point, preserving chain integrity while enabling reprocessing. Effective plastic recycling also demands meticulous **pre-sorting and cleaning**. Mixing incompatible plastic types or processing materials contaminated with adhesives, oils, or labels can severely impair the mechanical properties and purity of the recycled output. Proper cleaning and classification are therefore prerequisites for producing high-quality recycled plastic (Rios et al., 2007). These practices are integral to the operational framework of the Poly Pelletizer system, which aims to emulate industrial processing conditions while optimizing recyclability.

2.1 The Basics of Drying Plastic Pellets

When plastic pellets are exposed to ambient air, they readily absorb moisture due to their hygroscopic nature. This moisture uptake is driven by a vapor pressure differential between the polymer and its surroundings. Over time, water vapor diffuses into the polymer matrix until moisture equilibrium is achieved—at which point the internal moisture content of the pellet matches that of the surrounding environment, and the migration of additional water vapor effectively ceases (Longo and Gasparella, 2005). During this process, water molecules form strong intermolecular bonds with the polar regions of the polymer chains, as illustrated in Fig. 1. These hydrogen bonds contribute to the inherent difficulty of drying plastic pellets. Even trace levels of residual moisture can induce hydrolysis when the polymer is heated beyond its melt temperature, resulting in the scission of polymer chains and subsequent degradation of mechanical and processing properties (Longo and Gasparella, 2005).

The drying process of hygroscopic polymers, such as plastic pellets, is governed by four fundamental parameters:

i. Drying temperature,
ii. Dew point of the drying air,
iii. Drying time, and
iv. Airflow rate.

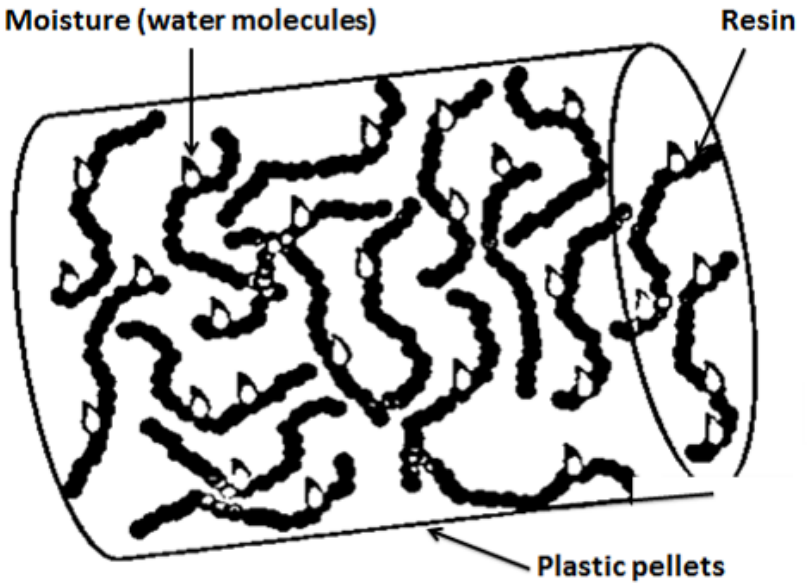

Fig. 1. Water Molecules Bond to the Plastic Polymer Chain

Among these, drying temperature is arguably the most critical factor. As the temperature of the polymer increases, molecular mobility within the pellet matrix intensifies, leading to a decrease in the intermolecular attraction between absorbed water molecules and the polymer chains. This elevated thermal energy disrupts the hydrogen bonding between the moisture and the polymer, facilitating the desorption and migration of water vapor toward the pellet surface and eventually into the surrounding airstream, as illustrated in Fig. 2 (Strumillo & Kudra, 1986; Martynenko & Vieira, 2023).

By carefully regulating temperature in conjunction with dew point and airflow, optimal moisture removal can be achieved without compromising the polymer's structural integrity or inducing thermal degradation (Loemba, 2022).

The temperature of the polymer exerts a profound influence on the diffusion rate of water molecules within the plastic matrix. As the temperature rises, the kinetic energy of the molecules increases, thereby diminishing the intermolecular attraction between the polymer chains and the water molecules. This reduction in bonding strength allows moisture to migrate more freely through the polymer structure. Achieving and maintaining the optimum drying temperature is essential to effective moisture removal. At elevated temperatures, drying occurs both more rapidly and more thoroughly. However, this must be balanced against the risk of thermal degradation and oxidative damage, which can arise if the polymer is exposed to excessively high temperatures. Conversely, if the drying temperature is too low, moisture removal proceeds inefficiently, as the polymer retains its affinity for water. The dew point temperature constitutes the second critical parameter in the drying process. It refers to the temperature at which air becomes saturated with moisture, leading to condensation. In other words, the dew point is the temperature at which the air's relative humidity reaches 100%. For instance, dew formation on grass during early summer mornings occurs because the ambient temperature drops below the dew point overnight, triggering condensation. In the context of polymer drying, the drying air is first dehumidified using desiccant materials that adsorb residual moisture, thereby achieving a very low dew point. The air is then heated to the target drying temperature, which dramatically reduces its relative humidity and substantially increases its capacity to absorb moisture. When plastic pellets are exposed to this low-dew point, high-temperature air—typically around 300°F (approximately 149°C)—a substantial vapor-pressure gradient is established between the interior of the pellet and the surrounding air. As the pellets reach the target temperature and the water-polymer interactions are sufficiently weakened, trapped water molecules migrate toward the surface, driven by the vapor pressure differential. Upon reaching the surface, these molecules are rapidly evacuated by the airstream, as depicted in Fig. 3.

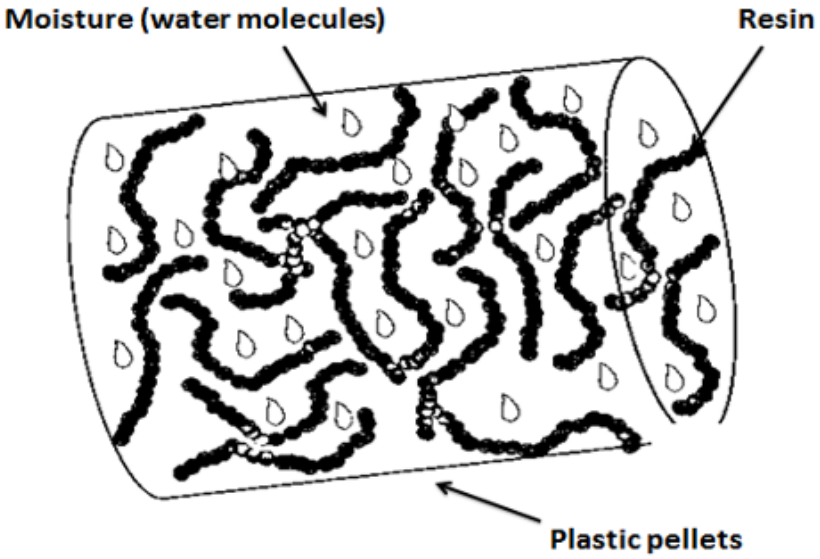

Fig. 2. Hot drying air loosen the bonds between moisture and the resin, allowing the molecules to move freely through the pellet

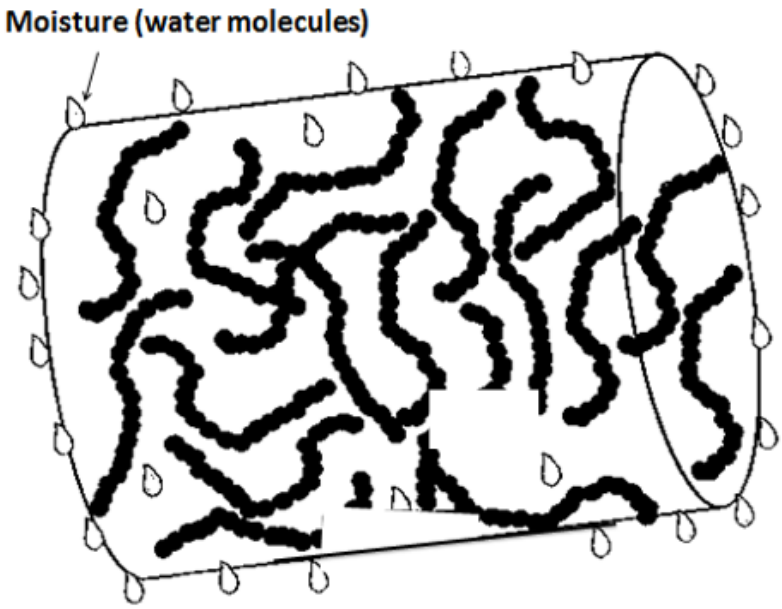

Fig. 3. Stream of dry air swept away the moisture content at the plastic pellets surface

The drying time, identified as the third fundamental parameter in the plastic pellet drying process, plays a critical role in ensuring effective moisture removal. Contrary to common perception, pellets do not dry instantaneously upon exposure to heated, low-dew point air. Once placed within the drying hopper, a sustained and consistent exposure is required to allow thermal energy from the surrounding air to penetrate the pellet surface and migrate toward its core (Thumsorn et al, 2011). Due to the inherently poor thermal conductivity of plastic pellets, this heat transfer process occurs gradually. Consequently, adequate time must be allotted for the heat to be absorbed and evenly distributed throughout the interior of the pellets. Importantly, the residence time of pellets in the drying hopper does not automatically equate to effective drying time. Effective drying time is defined as the duration during which the pellets are exposed to air maintained at the optimal drying temperature and dew point. Without this

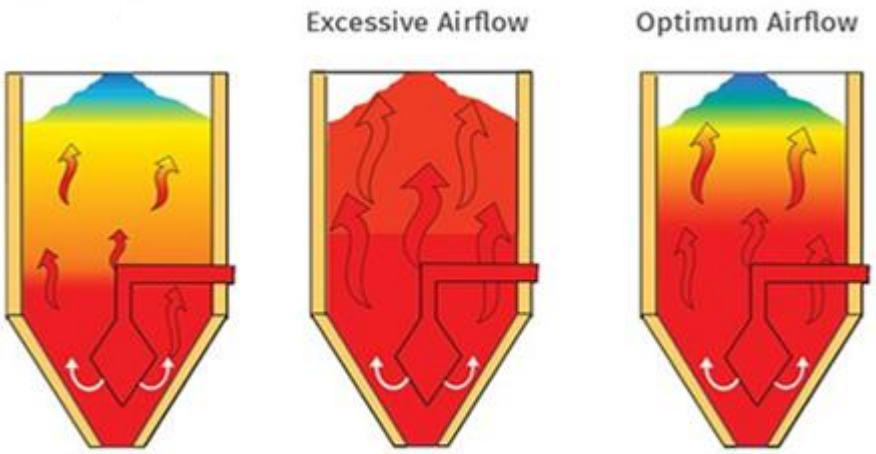

Fig. 4. The Importance of Proper Airflow: Insufficient airflow (left), Excessive airflow (center) and optimal airflow (right)

precise thermal and humidity control, drying efficiency is compromised, regardless of how long the material remains in the hopper (Thumsorn et al, 2011).

This relationship between airflow and drying efficiency is visually depicted in Fig. 4, which illustrates three airflow scenarios within a drying hopper: low, excessive, and optimal airflow. In the low airflow scenario, insufficient heated air reaches the material, resulting in inadequate drying time and poor moisture removal. Conversely, excessive airflow overheats the entire hopper content, leading to significant energy wastage as surplus heat is unnecessarily returned to the dryer. The optimum airflow condition, however, establishes a vertical temperature gradient, delivering sufficient drying time while efficiently utilizing the incoming cool material as a heat sink to reduce the return air temperature. This balance enhances both energy efficiency and material quality (Thumsorn et al, 2011).

2.2 Effect of Drying Time on Moisture Content

As drying time increases, the moisture content of a material generally decreases. Initially, moisture is removed rapidly during the constant rate period. As drying continues, the rate slows down during the falling rate period, where internal moisture must diffuse to the surface. Eventually, the material reaches its equilibrium moisture content, beyond which further drying has minimal effect and may cause damage or waste energy. Understanding this relationship is key to optimizing drying processes, preserving product quality, and improving energy efficiency.

3. AIR CIRCUITS AND OPERATIONAL PRINCIPLES OF A DEHUMIDIFYING PLASTIC PELLET DRYER

A well-engineered dehumidifying dryer integrates three essential air circuits: (i) a closed-loop drying-air circuit, (ii) a single-pass regeneration-air circuit, and (iii) a desiccant cooling circuit (Haynie, 2023). Prior to entering the drying hopper, the drying air undergoes dehumidification to achieve a low dew point and is subsequently heated to the selected drying temperature. As this heated, low-dew point air enters and diffuses throughout the hopper, it envelops every plastic pellet, transferring thermal energy and initiating the desorption of moisture from the hygroscopic polymer matrix. As the drying air ascends through the hopper, it gradually relinquishes heat to the pellets while simultaneously absorbing moisture liberated from the resin. The air exiting the hopper consequently exhibits a substantial increase in moisture content and a reduction in temperature (Sitompul, Istadi, and Sumardiono, 2003). Nonetheless, the air remains drier than ambient air, making a closed-loop configuration energetically advantageous. Return-air dew point temperatures in such systems typically range from 0°C to -29°C, whereas ambient dew points are significantly higher, necessitating reuse of return air for economic and thermodynamic efficiency (Fahad, 2023). The inclusion of a dust collector is vital for maintaining the long-term performance of the heat exchanger. Virgin plastic

pellets often carry fines, and reground scrap materials may contain even larger quantities. If unfiltered, these fines adhere to the heat exchanger's cooling coils, impeding thermal transfer and decreasing system efficiency over time (Dhodapkar, et al. 2009). Therefore, it is prudent to employ a dust collector upstream to mitigate coil fouling. Typical drying air temperatures fall within the range of 149°C to 177°C. Upon exit, the air has typically cooled to between 93°C and 121°C. Despite this reduction, the return air remains too hot to be reintroduced directly into the dryer due to its detrimental effect on desiccant performance. Optimal desiccant operation occurs within the return-air temperature range of 38°C to 54°C, wherein the desiccant may adsorb up to 15% of its own weight in moisture (Law and Mujumdar, 2012). Elevated return-air temperatures impair moisture adsorption and can result in desiccant degradation. Desiccant protection is critical to dryer longevity. The return-air filter—preceded by the dust collector—functions as a safeguard against fines. Should fines infiltrate the desiccant, they may cause airflow restriction, volatile release under heat, or permanent damage to the adsorption media. Thus, rigorous filtration is essential. The return-air filter, often the most maintenance-intensive component, must be cleaned or replaced based on the quantity of fines present, which can vary significantly depending on the feedstock composition (Novatec Inc., 2021). Regular monitoring and a tailored maintenance schedule are advisable. The drying-air blower is responsible for circulating air through the system and must supply sufficient pressure and flow to (a) overcome heat losses, (b) elevate incoming pellets from ambient temperature to 149–177°C, and (c) maintain adequate throughput through the hopper—even when drying high-load regrind materials with significant backpressure (20–30 in. H_2O).

The desiccant, typically composed of synthetic zeolite in the form of a molecular sieve, is the core of the dehumidifying dryer. Its function is to adsorb water from return air and reduce its dew point to a range of -34°C to -40°C (Mehare, et al. 2025). High-performance desiccants such as 13X zeolite are also capable of adsorbing organic compounds like acetaldehyde (AA), which is a concern in beverage bottle production due to its impact on flavor. Virgin pellets generally contain 1–3 ppm of AA, while reground pellets may exceed 10–15 ppm. Hence, the dryer must accommodate both water and volatile compound removal in such applications (Wellet, 2018). Heating of the drying air may be achieved using either electrical or natural gas-based systems. While electric heaters are simpler and less costly in initial outlay, natural gas may offer lower operational costs depending on regional utility rates. In gas-heated systems, indirect heat exchangers are imperative to prevent contamination of the drying air with combustion by-products, thereby preserving pellet quality. Similarly, in the regeneration-air circuit, ambient plant air is drawn, filtered, and heated in a single-pass system to purge accumulated moisture from the desiccant. The regeneration blower must provide sufficient airflow and pressure to raise the desiccant temperature to the factory-defined regeneration setpoint, thereby ensuring complete moisture desorption. The heated desiccant then releases the adsorbed water, which is vented to the atmosphere via an exhaust port (Mujumdar, 2007).

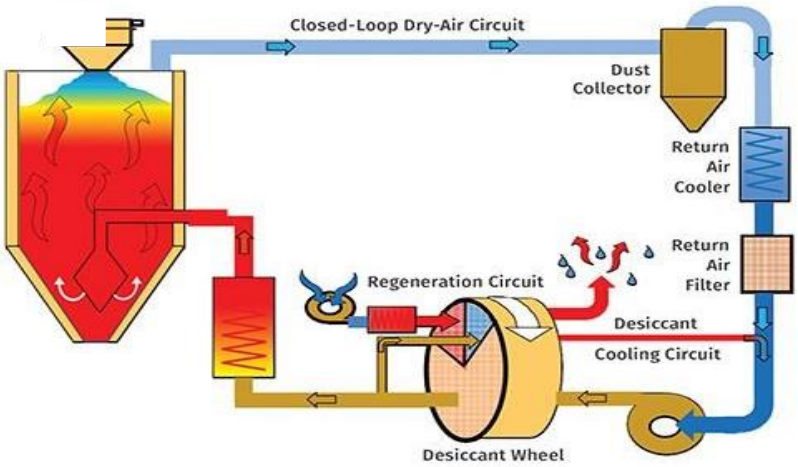

Fig. 5. Closed – Loop Drying-Air Circuit

4. DEHUMIDIFYING PLASTIC DRYER BED MODEL GOVERNING EQUATIONS

The equations are written for both fluid and porous region separately as shown in the model in Fig. 6 and then introduce proper boundary conditions at the interface for solutions. The fluid flow into the channel is assumed to be steady with regards to heat and mass transfer.

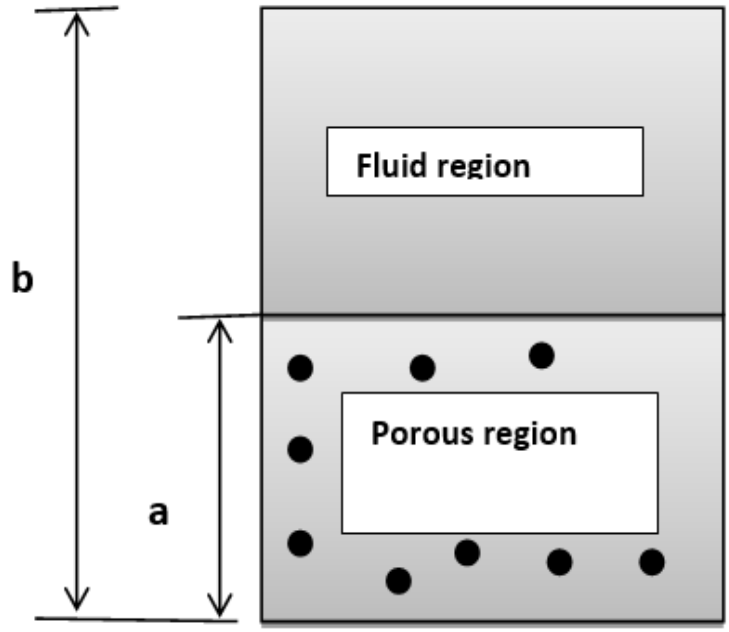

Fig. 6. Dehumidify Dryer model

The conservation equation governing mass, momentum, or energy transport within the porous medium of the dehumidifying bed can be expressed as follows:

$$\left(\frac{d^2u}{dy^2}\right)_{po} - \left(\frac{\sigma}{\psi}u\right)_{po} = \frac{1}{\mu}\Delta p \quad \text{……..} \quad (1)$$

$$\left[\left(\rho C_P\right)u_{po}\frac{dT}{dx}\right] = K_{po}\frac{d^2T_{po}}{dy^2} + \dot{q} \quad \text{……..} \quad (2)$$

$$u_{po}\frac{dm}{dx} = D_{po(v-a)}\frac{d^2m_{po}}{dy^2} + \frac{\dot{m}_{wv}}{\rho} \quad \text{……..} \quad (3)$$

The simplification of the energy transfer equation (2) was based on the dominant flow and temperature gradient directions observed in the geometry and configuration of the drying chamber. In forced-convection drying systems with unidirectional airflow, convective heat transfer tends to dominate in the primary flow direction (x-axis), while temperature gradients normal to the airflow (y-axis) are more effectively captured by conductive terms.

The conservation equation governing the fluid phase within the dehumidifying bed channel is expressed as follows:

$$\mu\left(\frac{d^2u}{dy^2}\right)_F = -\Delta p \quad \ldots\ldots\ldots\ldots\ldots\ldots\ldots\ldots\ldots\ldots\ldots\ldots\ldots\ldots\ldots\ldots\ldots\ldots\ldots\ldots \quad (4)$$

$$\left[u_F \frac{dT}{dx}\right] = \alpha_F \frac{d^2T_F}{dy^2} \quad \ldots\ldots\ldots\ldots\ldots\ldots\ldots\ldots\ldots\ldots\ldots\ldots\ldots\ldots\ldots\ldots\ldots\ldots\ldots\ldots\ldots\ldots \quad (5)$$

$$u_F \frac{dm}{dx} = D_{(v-a)} \frac{d^2m_F}{dy^2} \quad \ldots\ldots\ldots\ldots\ldots\ldots\ldots\ldots\ldots\ldots\ldots\ldots\ldots\ldots\ldots\ldots\ldots\ldots\ldots\ldots\ldots\ldots \quad (6)$$

The **source terms** in the conservation equations correspond to the **rate of water vapor generation** and the **heat release** due to moisture desorption from the pellets. These source terms can be mathematically represented as follows:

$$\dot{m}_{wv} = (\rho u)_{po}\, St_m \sum m_{po,s} - m_{po,b} \quad \ldots\ldots\ldots\ldots\ldots\ldots\ldots\ldots\ldots\ldots\ldots\ldots\ldots\ldots\ldots\ldots\ldots\ldots\ldots\ldots\ldots\ldots \quad (7)$$

$$\dot{q} = h_{ads}\left((\rho u)_{po}\, St_m \sum m_{po,s} - m_{po,b}\right) \quad \ldots\ldots\ldots\ldots\ldots\ldots\ldots\ldots\ldots\ldots\ldots\ldots\ldots\ldots\ldots\ldots\ldots\ldots\ldots\ldots\ldots\ldots \quad (8)$$

Where,

St_m = Stanton number for mass transfer between the solid and fluid in the void fraction

h_{ads} = enthalpy of the adsorption for the desiccant

Boundary conditions:

$$\text{At } y = 0, \quad u_{po} = 0, \quad \text{and} \quad K_m \frac{dT_{po}}{dy} = -q_L$$

$$\frac{dm_{po}}{dy} = 0 \quad \ldots\ldots\ldots\ldots\ldots\ldots\ldots\ldots\ldots\ldots\ldots\ldots\ldots\ldots\ldots\ldots\ldots\ldots\ldots\ldots\ldots\ldots \quad (9)$$

$$\text{At } y = b, \quad u_F = u_{po}, \quad \text{and} \quad \sigma \frac{du_f}{dy} = \frac{du_{po}}{dy}$$

$$T_F = T_{po,} \text{and} \quad \gamma \frac{dT_f}{dy} = \frac{dT_{po}}{dy}$$

$$m_F = m_{po,} \text{and} \quad \varepsilon \frac{dm_f}{dy} = \frac{dm_{po}}{dy} \quad \ldots\ldots\ldots\ldots\ldots\ldots\ldots\ldots\ldots\ldots\ldots\ldots\ldots\ldots\ldots\ldots\ldots\ldots\ldots\ldots\ldots\ldots \quad (10)$$

$$\text{At } y = a, \quad u_F = 0, \quad \text{and} \quad K_f \frac{dT_F}{dy} = q_V$$

$$\frac{dm_f}{dy} = 0 \quad \ldots\ldots\ldots\ldots\ldots\ldots\ldots\ldots\ldots\ldots\ldots\ldots\ldots\ldots\ldots\ldots\ldots\ldots\ldots\ldots\ldots\ldots \quad (11)$$

By performing **mass and energy balances** on a differential control volume element Δx along the axial direction of the dehumidifying bed channel, the following governing expressions are derived:

$$\frac{dT_b}{dx} = \frac{1}{\left(\rho C_P\right)_F u_b}\left[q_L\text{"} + q + b\dot{q}\right]$$

$$\frac{dm_b}{dx} = \frac{1}{\rho u}\frac{t_{po}}{t_c}\dot{m}_{wv} \quad \ldots\ldots\ldots\ldots\ldots\ldots\ldots\ldots\ldots\ldots\ldots\ldots\ldots\ldots \quad (12)$$

To simplify the analysis and generalize the behavior of the dehumidifying bed, the governing equations and associated boundary conditions were non-dimensionalized. This approach yields the following dimensionless form of the governing relation:

$$\text{as y tends to ay,} \qquad \Delta\text{p} \rightarrow \frac{\mu_F \alpha_F}{a^3}\Delta\text{p}$$

$$\text{as u tends to } \frac{\alpha_F u}{a}, \qquad \text{T} \rightarrow \frac{\left(q_L^{"} + q_U^{"}\right)a}{K_F}T \quad \ldots\ldots\ldots\ldots\ldots\ldots\ldots\ldots\ldots\ldots\ldots\ldots\ldots\ldots \quad (13)$$

The conservation equation 's scaling gives:

$$\left(\frac{d^2u}{dy^2}\right)_F = -\Delta P \quad \ldots\ldots\ldots\ldots\ldots\ldots\ldots\ldots\ldots\ldots\ldots\ldots\ldots\ldots \quad (14)$$

$$\left(\frac{d^2T}{dy^2}\right)_F = \frac{u_F}{u_b}\left(1+\dot{q}\right) \quad \ldots\ldots\ldots\ldots\ldots\ldots\ldots\ldots\ldots\ldots\ldots\ldots\ldots\ldots\ldots\ldots\ldots\ldots\ldots\ldots \quad (15)$$

$$\frac{d^2m_F}{dy^2} = \varepsilon\dot{M}_{wv}\left(\frac{u_F}{u_b}\right)\left(\frac{t_{po}}{t_c}\right) \quad \ldots\ldots\ldots\ldots\ldots\ldots\ldots\ldots\ldots\ldots\ldots\ldots\ldots\ldots\ldots\ldots\ldots\ldots\ldots\ldots \quad (16)$$

$$\frac{d^2u_{po}}{dy^2} - \left[\frac{\frac{\mu_F}{\mu_m}}{\frac{\psi}{b^2}\left(\frac{t_{po}}{t_c}\right)^2}\right]u_{po} = -\frac{\mu_F}{\mu_m}\Delta p \quad \ldots\ldots\ldots\ldots\ldots\ldots\ldots\ldots\ldots\ldots\ldots\ldots\ldots\ldots\ldots\ldots\ldots\ldots\ldots\ldots \quad (17)$$

$$\frac{d^2T_{po}}{dy^2} = \frac{K_F}{K_m}\left[\left(\frac{u_{po}}{u_b}\right)\left(1+\dot{q}\right) - \frac{t_c\dot{q}}{t_{po}}\right] \quad \ldots\ldots\ldots\ldots\ldots\ldots\ldots\ldots\ldots\ldots\ldots\ldots\ldots\ldots\ldots\ldots\ldots\ldots\ldots\ldots \quad (18)$$

$$\frac{d^2m_{po}}{dy^2} = \dot{M}_{wv}\left[\left(\frac{u_F}{u_b}\right)\left(\frac{t_{po}}{t_c}\right) - 1\right] \quad \ldots\ldots\ldots\ldots\ldots\ldots\ldots\ldots\ldots\ldots\ldots\ldots\ldots\ldots\ldots\ldots\ldots\ldots\ldots\ldots \quad (19)$$

where,

$$\dot{M}_{wv} = \frac{\dot{m}_{wv} a^2}{\rho D_{po(v-a)}} \quad \text{(20)}$$

$$\dot{q} = \frac{bq}{q_L^" + q_U^"} \quad \text{(21)}$$

Since, $q = Q_{ad}\dot{m}_{wv} = \frac{\rho Q_{ad} D_{v-a}}{a^2}\dot{M}_{wv}$ (22)

$$\therefore \dot{q} = \frac{b\dot{M}_{wv}\rho Q_{ad} D_{po(v-a)}}{\left(q_L^" + q_U^"\right) a^2} \quad \text{(23)}$$

The total fluid velocity across the entire dehumidifying bed channel can be expressed as:

$$u_b = \int_0^{\eta} u_{po} dy + \int_{\eta}^{1} u_F dy \quad \text{(24)}$$

Applying factor analysis, the boundary conditions transform into the following expressions:

at y = 0, $u_{po} = 0,$

$$\frac{dT_{po}}{dy} = -\left(\frac{\frac{K_F}{K_m}\left(\frac{q_L}{q_V}\right)}{1 + \frac{q_L}{q_V}}\right)$$

$$\frac{dm_{po}}{dy} = 0 \quad \text{(25)}$$

at y = η,

$u_F = u_{po},\quad \sigma\frac{du_F}{dy} = \frac{du_{po}}{dy}$

$T_F = T_{po,}$ and $\gamma\frac{dT_f}{dy} = \frac{dT_{po}}{dy}$

$m_F = m_{po,}$ and $\varepsilon\frac{dm_F}{dy} = \frac{dm_{po}}{dy}$ (26)

At y = 1, $u_F = 0,$ and $\frac{dT_F}{dy} = \frac{1}{1 + \frac{q_L}{q_U}}$

$$\frac{dm_F}{dy} = 0 \quad \text{(27)}$$

Therefore, the dimensionless rate of water vapour production gives:

$$\dot{M}_{wv} = \frac{a^2\left(\rho u_{po} St_m\right)}{\rho D_{po(v-a)}} \sum\left(K_1 T_{po} + K_2 - m_{po}\right) \quad \ldots\ldots\ldots\ldots \quad (28)$$

5. RESULTS AND DISCUSSION

The fluid flow within the dehumidifying bed is governed by a set of equations whose solutions were derived through an analytical approach. Initially, the velocity field and bulk velocity were solved, which subsequently enabled the resolution of the energy and species mass transport equations. Ultimately, the bulk temperature and bulk water vapor mass fraction were determined. The velocity distribution in the fluid region is expressed as follows:

$$u_F = -\frac{\Delta P}{2}\left(y^2 - 1\right) + c_1\left(y - 1\right) \quad \ldots\ldots\ldots\ldots \quad (29)$$

Where, $c_1 = G_F \Delta p$

$$\text{and } G_F = \left\{\frac{t_{po}}{t_c} - 1 - \frac{\tanh\left(\beta\frac{t_{po}}{t_c}\right)}{\beta}\sigma\right\}^{-1}\left[\left\{\left(\frac{t_{po}}{t_c}\right)^2 - 1\right\}2 + \frac{\psi}{b^2}\left(\frac{t_{po}}{t_c}\right) - \sigma\left(\frac{t_{po}}{t_c}\right)\frac{\tanh\left(\beta\frac{t_{po}}{t_c}\right)}{\beta}\right]$$

$$-\left(\frac{t_{po}}{t_c}\right)\frac{\psi}{b^2}^2 Cosh\left(\beta\frac{t_{po}}{t_c}\right) + \frac{\tanh\left(\beta\frac{t_{po}}{t_c}\right)}{\beta}\beta\left(\frac{\psi}{b^2}\right)^2 Sinh\left(\beta\frac{t_{po}}{t_c}\right) \quad \ldots\ldots\ldots\ldots \quad (30)$$

The velocity distribution within the porous region was derived and is expressed as follows:

$$u_{po} = \Delta p \delta\left(\frac{t_{po}}{t_c}\right)^2\left[1 - Cosh\left(\beta y\right)\right] + c_2 Sinh\left(\beta y\right) \quad \ldots\ldots\ldots\ldots \quad (31)$$

Where, $c_2 = G_{po} \Delta p$

$$G_{po} = \frac{\sigma\left(\frac{\tanh\left(\beta\frac{t_{po}}{t_c}\right)}{\beta}\right)\left(G_F - \frac{t_{po}}{t_c}\right)}{Sinh\left(\beta\right)} + \frac{\psi}{b^2}\left(\frac{t_{po}}{t_c}\right)^2\frac{\tanh\left(\beta\frac{t_{po}}{t_c}\right)}{\beta}\beta \quad \ldots\ldots\ldots\ldots \quad (32)$$

$$\text{Where, } \beta = \sqrt{\frac{\alpha\left(\frac{t_{po}}{t_c}\right)^2}{\frac{\psi}{b^2}}} \quad \ldots\ldots\ldots\ldots \quad (33)$$

Therefore, the solution for the velocity in the fluid region, expressed in terms of the dimensionless bulk velocity, is given by:

$$\frac{u_F}{u_b} = \left[z_F + z_{po} \right]^{-1} \left[-\frac{y^2}{2} + G_F \right] \quad \text{(34)}$$

where,

$$z_F = \int_{\eta}^{1} \left\{ -\frac{y^2}{2} + G_F y + \frac{1}{2} - G_F \right\} dy \quad \text{(35)}$$

Similarly, the solution for the velocity in the porous region, expressed in terms of the dimensionless bulk velocity, is given by:

$$\frac{u_{po}}{u_b} = \left[z_F + z_{po} \right]^{-1} \left[\frac{\psi}{b^2} \left(\frac{t_{po}}{t_c} \right)^2 \left\{ 1 - Cosh(\beta y) \right\} + G_{po} Sinh(\beta y) \right] \quad \text{(36)}$$

where,

$$z_{po} = \int_{0}^{\eta} \left\{ -\frac{\psi}{b^2} \left(\frac{t_{po}}{t_c} \right)^2 Cosh(\beta y) + G_{po} Sinh(\beta y) + \frac{\psi}{b^2} \left(\frac{t_{po}}{t_c} \right) \right\} dy \quad \text{(37)}$$

The mass fraction of water vapor in the fluid region can be expressed as follows:

$$m_F = \varepsilon \dot{M}_{wv} \frac{t_{po}}{t_c} \left[z_F + z_{po} \right]^{-1} \left\{ \begin{array}{l} -\dfrac{\left(y^4 - \left(\frac{t_{po}}{t_c} \right)^4 \right)}{24} + \dfrac{G_F \dfrac{y^3}{\left(\frac{t_{po}}{t_c} \right)^3}}{6} + \dfrac{\left(1 - 2G_F \right) \left(y^2 - \left(\frac{t_{po}}{t_c} \right)^2 \right)}{4} + \\ + \dfrac{\left(2 - 3G_F \right) \left(y - \frac{t_{po}}{t_c} \right)}{6} \end{array} \right\} + m_i \quad \text{(38)}$$

Similarly, the mass fraction of water vapor in the porous region can be expressed as:

$$m_{po} = \dot{M}_{wv} \frac{t_{po}}{t_c} \left[z_F + z_{po} \right]^{-1} \left\{ \begin{array}{l} -\dfrac{\left(\frac{\psi}{b^2} \left(\frac{t_{po}}{t_c} \right)^2 \left(y^2 - \left(\frac{t_{po}}{t_c} \right)^2 \right) \right)}{2} - \\ \dfrac{G_{po} \left(y - \frac{t_{po}}{t_c} \right)}{\beta} - \dfrac{\frac{\psi}{b^2} \left(\frac{t_{po}}{t_c} \right)^2}{\beta^2} \left(Cosh(\beta y) - Cosh\left(\beta \frac{t_{po}}{t_c} \right) \right) + \\ + \dfrac{G_{po}}{\beta^2} \left(\left(Sinh(\beta y) - Sinh\left(\beta \frac{t_{po}}{t_c} \right) \right) \right) \end{array} \right\} - \frac{y^2 - \left(\frac{t_{po}}{t_c} \right)^2}{2} + m_i \quad \text{(39)}$$

$$\text{when } y = \frac{t_{po}}{t_c}, m_F = m_{po} = m_i \quad (40)$$

By performing a double integration of the energy equations, the temperature distribution within the fluid region was derived as follows:

$$T_F = (1+\dot{q})\left[z_F + z_{po}\right]^{-1}\left[\frac{\left(y^4 - \left(\frac{t_{po}}{t_c}\right)^4\right)}{24} + \frac{G_F \frac{y^3}{\left(\frac{t_{po}}{t_c}\right)^3}}{6} + \frac{(1-2G_F)\left(y^2 - \left(\frac{t_{po}}{t_c}\right)^2\right)}{4} + \frac{(2-3G_F)\left(y - \frac{t_{po}}{t_c}\right)}{6}\right] + \frac{y - \frac{t_{po}}{t_c}}{1+\frac{q_L}{q_U}} + T_i \quad (41)$$

$$T_{po} = \frac{K_F}{K_m}(1+\dot{q})\left[z_F + z_{po}\right]^{-1}\left\{\frac{\left(\frac{\psi}{b^2}\left(\frac{t_{po}}{t_c}\right)^2\left(y^2 - \left(\frac{t_{po}}{t_c}\right)^2\right)\right)}{2} - \frac{1}{\beta^2}\left(Cosh(\beta y) - Cosh\left(\beta\frac{t_{po}}{t_c}\right)\right) + \frac{G_{po}}{\beta^2}\left(\left(Sinh(\beta y) - Sinh\left(\beta\frac{t_{po}}{t_c}\right)\right)\right) - \frac{y^2 - \left(\frac{t_{po}}{t_c}\right)}{2\left(\frac{t_{po}}{t_c}\right)}\dot{q}\left(\frac{\psi}{b^2}\right)\right\} - \frac{\frac{\psi}{b^2}\left(\frac{q_L}{q_U}\right)\left(y - \frac{t_{po}}{t_c}\right)}{1+\frac{q_L}{q_U}} + T_i \quad (42)$$

$$\therefore T_F = T_{po} = T_i \quad \text{when} \quad z = \frac{t_{po}}{t_c} \quad (43)$$

The water vapor production rate within the channel was determined using the following equation:

$$\dot{M}_{wv} = \frac{u_{b,po}a^2}{D_{v-a}} St_m \sum\left[K_1 T_{po,b} + K_2 - m_{po,b}\right] \quad (44)$$

Additionally, the internal heat generation rate within the channel was determined using the following equation:

$$\dot{q} = \frac{bQ_{ad}}{q_L + q_U}\rho u_{b,po} St_m \sum\left[K_1 T_{po,b} + K_2 - m_{po,b}\right] \quad (45)$$

The mass fraction of the fluid in the porous region can be expressed as follows:

$$\frac{dm_{po,b}}{dx} = \frac{\frac{t_{po}}{t_c}}{\rho u_b}\rho u_{b,po} St_m \sum\left[K_1 T_{po,b} + K_2 - m_{po,b}\right] \quad (46)$$

Similarly, the bulk temperature of the fluid in the porous region can be expressed as:

$$\frac{dT_{po,b}}{dx} = \frac{\frac{t_{po}}{q_L + q_U}}{\rho C_P u_b a} + \frac{Q_{ad}}{\rho C_P u_b a} \rho u_{b,po} St_m \sum \left[K_1 T_{po,b} + K_2 - m_{po,b} \right] \quad \text{.....} \quad (47)$$

Equations (46) and (47) can ultimately be solved numerically to obtain the governing relations for the temperature and mass fraction of the fluid within the porous region of the dehumidifying bed dryer, thereby facilitating the dehumidification of plastics. Furthermore, an expression for the Sherwood number, characterizing the mass transfer from the porous region to the fluid region of the dehumidifying bed channel, can be derived based on the solutions to the temperature and mass transfer equations within the bed.

$$Sh = \frac{k}{a\rho D_{v-a}} = \frac{m_{b,F} - m_i}{\frac{dm_F}{dy}} \quad \text{when y} = \frac{t_{po}}{t_c} \quad \text{.....} \quad (48)$$

Fig. 7 illustrates the moisture-loss analysis for a dehumidifying dryer bed. During static drying, small samples of the plastic pellets were taken from the hopper every hour to measure residual moisture. The drying parameters are detailed in the chart accompanying the figure. A significant reduction in residual moisture occurred within the first hour of drying, dropping sharply from 0.18% to 0.04%. After this initial phase, the rate of moisture loss slowed considerably, requiring an additional four hours to reduce moisture levels below the target threshold of 0.005%. Airflow in a dehumidifying dryer is a critical drying parameter because it serves as the medium that transfers heated, low-dew point air from the dryer to the pellets in the drying hopper. Insufficient airflow fails to deliver enough heat to the pellets, preventing the maintenance of the desired vertical temperature profile and, consequently, the required drying time. Conversely, excessive airflow results in too much heat being transferred to the drying hopper. Heat not absorbed by the pellets escapes with the return air, leading to elevated return-air temperatures, decreased desiccant efficiency, wasted energy, higher operating costs, and potential damage to the process-air blower. The necessary airflow volume varies depending on factors such as the initial pellet temperature, drying hopper design, heat losses within the system, and throughput rate (kg/hr). Adequate airflow must be maintained to keep pellets at the target drying temperature for the prescribed drying duration.

Although the data presented in Fig. 7 were originally obtained through experimental measurements, a comparative analysis was conducted between the experimental moisture content values and those calculated using Equation (46). The resulting comparison demonstrates a strong correlation between the experimental and modeled data, thereby providing additional validation for the adequacy and reliability of the proposed mathematical model.

At the end of the regeneration cycle, the desiccant reaches an elevated temperature and very low residual moisture content. Before re-entering the drying-air circuit, the desiccant must be cooled, as shown in Fig. 8. Introducing hot desiccant directly into the process-air stream results in poor moisture adsorption because the high temperature prevents effective moisture removal from the return air. Consequently, high-dew point air is recirculated into the drying hopper, reducing drying efficiency. A small, controlled volume of air from the drying-air circuit is used to cool the desiccant in the cooling position. Some older dryer designs use ambient air for cooling, which risks loading the desiccant with moisture during cooling as its temperature drops, impairing performance.

Since the return air already has a low moisture content (due to prior drying), it prevents reintroducing moisture into the desiccant during cooling. This maintains the desiccant's dryness and adsorption capacity, ensuring better overall drying efficiency. Using ambient air for cooling risks exposing the desiccant to variable and often higher moisture levels, which can degrade its performance by prematurely saturating it before it even re-enters the drying process. So, the slipstream cooling method helps maintain a consistently low dew point in the drying circuit and optimizes the energy efficiency and effectiveness of the dehumidifying dryer system.

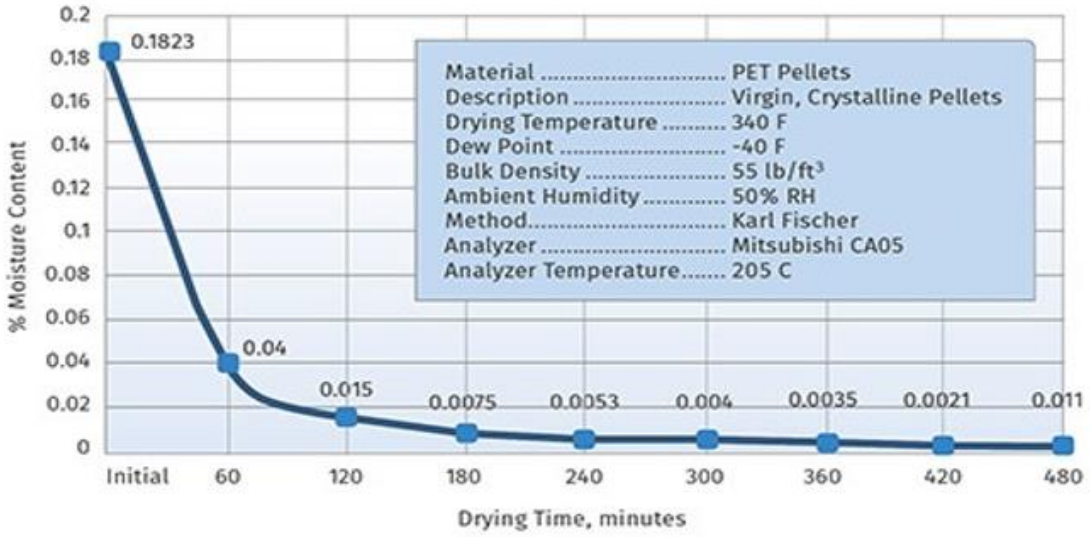

Fig. 7. Effects of drying time on moisture content

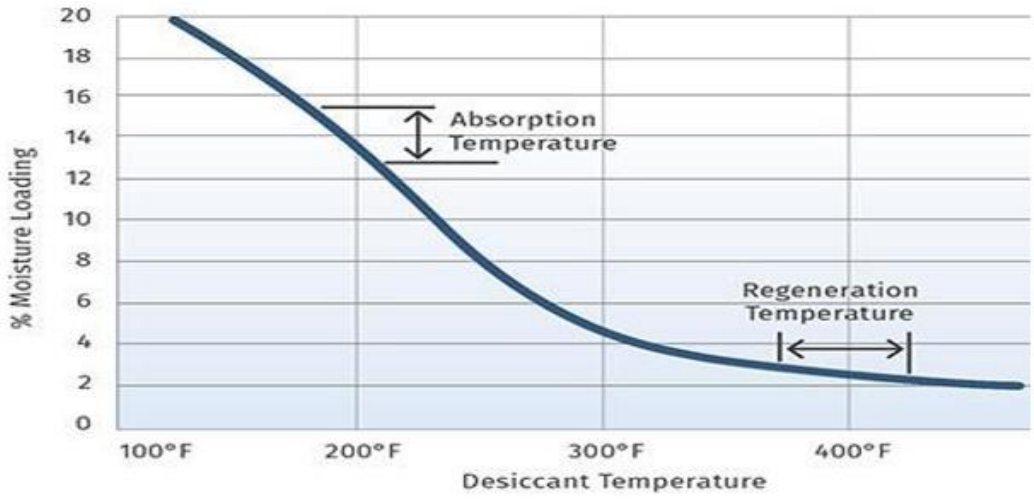

Fig. 8. Effects of Percentage Moisture Loading on Desiccant Temperature

6. CONCLUSION

A comprehensive numerical solution for the coupled heat and mass transfer phenomena within the fluid flow channel of a dehumidifying dryer was formulated and rigorously analyzed. The physical model conceptualized the system as a dual-region channel, with the lower portion constituted by a porous medium representing the dehumidifying bed. The derived analytical solutions provide spatially resolved distributions of fluid temperature and water vapor mass fraction throughout the dryer channel. This theoretical framework enables detailed sensitivity analyses concerning critical transport parameters, including the fluid-to-solid mass transfer coefficient and the water vapor-to-air mass diffusivity within the channel, thereby facilitating an assessment of their respective influences on system performance and the accuracy of parameterization. Moreover, the integrated solutions of the governing equations and the species mixture content dynamics afford a robust basis for predicting the transient thermal and moisture response characteristics of the drying system. Further, the empirical moisture-loss characterization of the dryer bed, coupled with a rigorous evaluation of airflow dynamics, substantiates airflow as a pivotal drying parameter. It was conclusively demonstrated that sustaining an optimal volumetric airflow through the drying hopper is essential to maintain pellet

temperatures within the prescribed drying range over sufficient residence times, thereby ensuring effective moisture removal and process efficiency.

DISCLAIMER (ARTIFICIAL INTELLIGENCE)

Author(s) hereby declare that NO generative AI technologies such as Large Language Models (ChatGPT, COPILOT, etc.) and text-to-image generators have been used during the writing or editing of this manuscript.

COMPETING INTERESTS

Author has declared that they have no known competing financial interests OR non-financial interests OR personal relationships that could have appeared to influence the work reported in this paper.

REFERENCES

Cuče, P. M., Yılmaz, Y. N., & Cuče, E. (2025). A comprehensive review on rotary desiccant wheel systems: The future of smart building climate control. *Journal of Thermal Analysis and Calorimetry*. https://doi.org/10.1007/s10973-025-14362-x

De Antonellis, S., Smith, J., Brown, L., & Garcia, M. (2012). Simulation and energy efficiency analysis of desiccant wheel systems in hybrid drying. *Applied Thermal Engineering, 37*, 318–326. https://www.sciencedirect.com/science/article/pii/S0360544211007390

Dhodapkar, S., Trottier, R., & Smith, B. (2009). Measuring dust and fines in polymer pellets. *Chemical Engineering*. https://www.scribd.com/document/332074249/Measuring-Dust-and-Fines-in-Polymer-Pellets

Fahad, F. G., Al-Humairi, S. T., Al-Ezzi, A. T., Majdi, H. S., Sultan, A. J., Alhuzaymi, T. M., & Aljuwaya, T. M. (2023). Advancements in liquid desiccant technologies: A comprehensive review of materials, systems, and applications. *Sustainability, 15*(18), 14021. https://doi.org/10.3390/su151814021

Ge, T. S., Li, Y., Wang, R. Z., & Dai, Y. J. (2008). A review of the mathematical models for predicting rotary desiccant wheel. *Renewable and Sustainable Energy Reviews, 12*(6), 1485–1528.

Haynie, M. (2023). *Best Practices for Effective Polymer Drying*. Novatec, Inc. https://www.novatec.com/wp-content/uploads/2023/04/Best-Practices-for-Effective-Polymer-Drying.pdf

Keey, R. B. (1992). *Drying of Loose and Particulate Materials*. CRC Press. https://books.google.com/books?hl=en&lr=&id=CYELHT3DQuEC&oi=fnd&pg=PR9&dq=Drying+of+Loose+and+Particulate+Materials&ots=dT1whoz_vM&sig=5dw_8zm7dncZbnj9zzKBlMeEkcE

Law, C. L., & Mujumdar, A. S. (2012). Energy saving in drying processes. In *Recent Advances in Sustainable Process Design and Optimization* (pp. 577–591). (With CDROM).

Loemba, A. B. T. (2022). Comprehensive assessment of heat pump dryers for agricultural products. *Energy Science & Engineering, 11*(8), 2985–3014. https://scijournals.onlinelibrary.wiley.com/doi/abs/10.1002/ese3.1326

Longo, G. A., & Gasparella, A. (2005). Experimental and theoretical analysis of heat and mass transfer in a packed column dehumidifier/regenerator with liquid desiccant. *International Journal of Heat and Mass Transfer, 48*(3–4), 5240. https://doi.org/10.1016/j.ijheatmasstransfer.2005.07.011

Martynenko, A. A., & Vieira, G. N. A. (2023). Sustainability of drying technologies: System analysis. *Sustainable Food Technology, 1*(1), 629–640. https://pubs.rsc.org/en/content/articlehtml/2023/fb/d3fb00080j

Mato, Y., Isobe, T., Takada, H., Kanehiro, H., Ohtake, C., & Kaminuma, T. (2001). Plastic resin pellets as a transport medium for toxic chemicals in the marine environment. *Environmental Science & Technology, 35*(2), 318–324. https://pubs.acs.org/doi/abs/10.1021/es0010498

Mehare, H. B., Hussain, T., Zia, M. A., & Saleem, S. (2025). Performance evaluation of a rotary dehumidifier with molecular sieve desiccant using coupled regeneration mode: Experimental investigation. *Energy and Built Environment, 6*(2), 219–229.

Mujumdar, A. S. (2007). *Handbook of Industrial Drying*. CRC Press. https://www.taylorfrancis.com/books/mono/10.1201/9781420017618/handbook-industrial-drying-arun-mujumdar

Novatec, Inc. (2021). *Resin dryer maintenance: How to maximize dryer uptime and efficiency*. Resin Dryer Maintenance - Plastic Knowledge Center.

Rigby, S. P. (2025). Modelling and simulation of surface diffusion in porous adsorbents. *Micromaterials, 8*(2), 31. https://doi.org/10.3390/micromaterials8020031

Rios, L. M., Moore, C., & Jones, P. R. (2007). Persistent organic pollutants carried by synthetic polymers in the ocean environment. *Marine Pollution Bulletin, 54*(8), 1230–1237. https://www.sciencedirect.com/science/article/pii/S0025326X07001324

Ruivo, C. R., Costa, J. J., & Figueiredo, A. R. (2009). Validity of pseudo-gas-side-controlled models to predict the behaviour of desiccant matrices. *International Journal of Thermal Sciences, 48*(11), 2171–2178.

Santos, A. A. d. L., Leal, G. F., Marques, M. R., Reis, L. C. C., Junqueira, J. R. d. J., Macedo, L. L., & Corrêa, J. L. G. (2025). Emerging drying technologies and their impact on bioactive compounds. *Applied Sciences, 15*(12), 6653. https://www.mdpi.com/2076-3417/15/12/6653

Sitompul, J. P., Istadi, & Sumardiono, S. (2003). Modeling and simulation of momentum, heat, and mass transfer in a deep bed grain dryer. *Drying Technology, 21*(2), 217–229. https://doi.org/10.1081/DRT-120017744

Strumillo, C., & Kudra, T. (1986). *Drying: Principles, Applications and Design*. Gordon and Breach Science. https://books.google.com/books?hl=en&lr=&id=rDSVDACG6GAC&oi=fnd&pg=PA1&dq=Drying:+Principles,+Applications+and+Design&ots=P61DeiiSwN&sig=WDXxAH7JDfg4Af5j3RPiBXz8cTI

Talsness, C. E., Andrade, A. J. M., Kuriyama, S. N., Taylor, J. A., & vom Saal, F. S. (2009). Components of plastic: Experimental studies in animals and relevance for human health. *Philosophical Transactions of the Royal Society B: Biological Sciences, 364*(1526), 2079–2096. https://royalsocietypublishing.org/doi/abs/10.1098/rstb.2008.0281

Welle, F. (2018). Migration of acetaldehyde from PET bottles into natural mineral water. *Reference Module in Food Science*. Elsevier. https://www.sciencedirect.com/science/article/pii/B9780128140456000832

Wong, E. H., & Park, S. B. (2016). Moisture diffusion modeling–A critical review. *Microelectronics Reliability, 65*, 318–326.

Ying, T., & Spang, E. S. (2024). Paddy drying technologies: A review of existing literature on energy consumption. *Processes, 12*(3), 532. https://www.mdpi.com/2227-9717/12/3/532

Peer-review history:
The peer review history for this paper can be accessed here:
https://pr.sdiarticle5.com/review-history/140958